ISSN 0027-1314, Moscow University Chemistry Bulletin, 2008, Vol. 63, No. 5, pp. 245–249. © Allerton Press, Inc., 2008.
Original Russian Text © A.L. Voskov, I.A. Uspenskaya, 2008, published in Vestnik Moskovskogo Universiteta. Khimiya, 2008, No. 5, pp. 295–299.

Calculation of Ln–Ba (Ln = Gd, Pr, Nd, and Sm) Phase Diagrams

A. L. Voskov and I. A. Uspenskaya

Department of Physical Chemistry
e-mail: ira@td.chem.msu.ru

Received November 12, 2007

Abstract—A thermodynamic model of liquid was suggested and Ln–Ba (Ln = Gd, Pr, Nd, and Sm) phase diagrams were calculated on the basis of generalization of literature data on thermodynamic properties and phase equilibria in lanthanide–barium metallic systems. The interaction parameter of $Gd_{1-x}Ba_x$ regular melt was estimated on the assumption of a proportionality between the particle–particle interaction energies of liquid lanthanide and liquid barium, on the one hand, and the lanthanide radius, on the other.

DOI: 10.3103/S0027131408050027

This work continues our studies [1–4] into the optimization of phase diagrams that constitute the base of some functional ceramics (oxygen pickups, high-temperature superconductors, magnets, and others). Experimental phase diagram data for most Ln–Ba binary systems (where Ln stands for a lanthanide) are incomplete; for the Gd–Ba system, they are nonexistent. Therefore, calculation of phase diagrams for these systems is pertinent.

Ln–Ba Binary Phase Diagrams

Experimentally, phase diagrams were studied for the La–Ba, Pr–Ba, Nd–Ba, Sm–Ba, Eu–Ba, and Yb–Ba systems. A tervalent lanthanide (La, Pr, Nd, or Sm) and barium form two immiscible liquids; the relevant phase diagrams feature an exsolution dome, a eutectic, and a monotectic [5–8]. Some divalent lanthanides (Eu and Yb) form complete solid and liquid solutions with barium; the behavior of cerium is still unknown, but presumably it more closely resembles tervalent lanthanides [9].

Phase equilibrium data for Ln–Ba systems are scarce; in some cases, eutectic and monotectic temperatures and component miscibility have been determined. Tables 1 and 2 compile the available data.

The melting temperatures of lanthanides and barium vary within several degrees from study to study; in

Table 1. Coordinates of singular points in Ln–Ba phase diagrams (experimental data)

Element	Melting	Monotectic		Eutectic		Source
	T_m(Ln), K	T, K	x_{Ba}, at %	T, K	x_{Ba}, at %	
Pr	1207	1203	–	–	–	[6]
Nd	1297	1283	4	963	90.0	[7]
Sm	1346	1293	1	963	99.7	[8]

Table 2. Miscibility of barium and lanthanides

Element	Ba in Ln		Ln in Ba		Source
	T, K	x_{Ba}, at %	T, K	x_{Ba}, at %	
Pr	–	–	–	–	[6]
Nd	1283	1.5	963	~3	[7]
	873	1.0	873	~2	
Sm	1293	0.7	~983	~0.1	[8]

Table 3. Interaction parameters and coordinates of singular points of Ln–Ba phase diagrams

Element	g_{00}, J/mol	r_{at}, pm [10]	$T_{ph\ tr}$, K	T_m, K	Monotectic		Eutectic	
					T, K	x_{Ba}, at %	T, K	x_{Ba}, at %
Pr	60000	182.8	1068	1204	1200	0.3	–	–
Nd	52500	182.1	1128	1289	1275	0.8	998	99.9
Sm	38250	180.2	1190	1345	1292	3.5	992	99.3

some cases (for Pr–Ba and Nd–Ba), the variation range is commensurate with the difference between the lanthanide melting temperature and monotectic temperature. Therefore, to diminish the systematic error, we did not use eutectic and monotectic temperatures; rather, we used the differences between these temperatures and the lanthanide and barium melting temperatures, respectively. In other words, we performed equalization with respect to reference points, as in [9]. Table 3 lists the revised monotectic temperatures.

The solid miscibility of barium and tervalent lanthanides is small; in view of its smallness and the paucity of experimental data, we ignored it in thermodynamic modeling of phases for Ln–Ba systems in this work.

Thermodynamic Model of Liquid

We used the regular solution model to describe the thermodynamic properties of Gd–Ba melts. The temperature and concentration dependence of the Gibbs energy of mixing in this case is

$$\Delta_{mix}G(T, x) = RT[(1-x)\ln(1-x) + x\ln x] + g_{00}x(1-x).$$

In finding the parameter g_{00} for $Ln_{1-x}Ba_x$ melts, we used the monotectic temperatures of the Ln–Ba (Ln = Pr, Nd, and Sm) systems. The monotectic temperatures in these systems were measured with the highest accuracy, whereas eutectic compositions have not been determined experimentally and eutectic temperatures are very close to the barium melting point. In view of the high chemical reactivity of barium, it is reasonable to suggest that all measurements near the pure barium point have a far greater error than in the lanthanide-rich compositions.

The numerical values of the melt interaction parameters were estimated proceeding from equilibrium con-

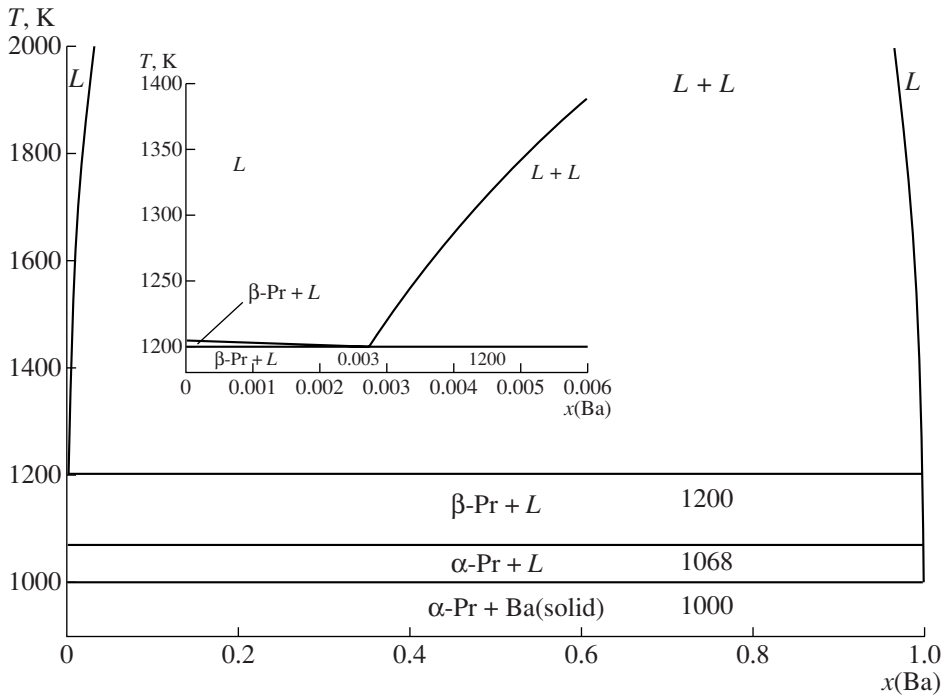

Fig. 1. Pr–Ba phase diagram.

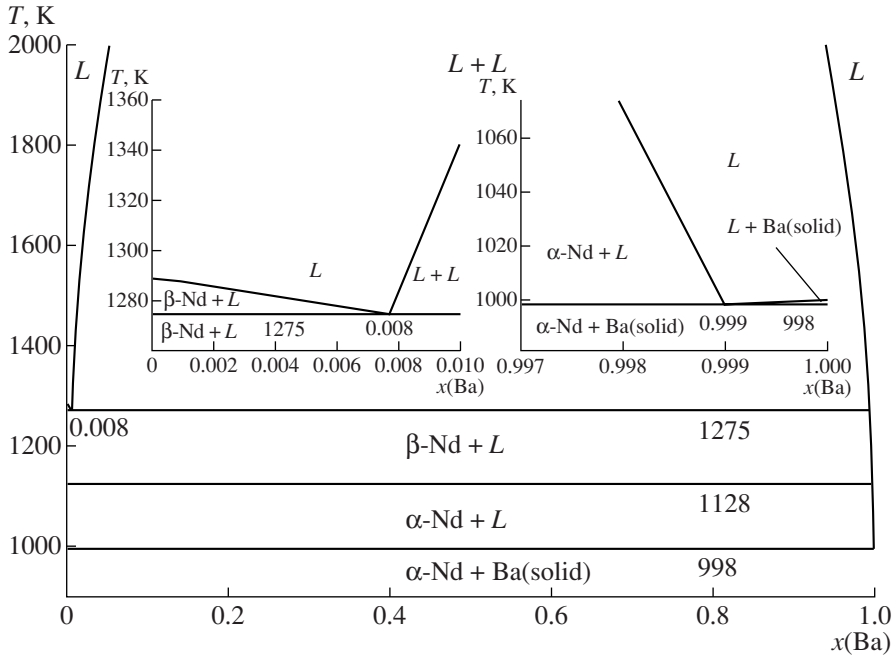

Fig. 2. Nd–Ba phase diagram.

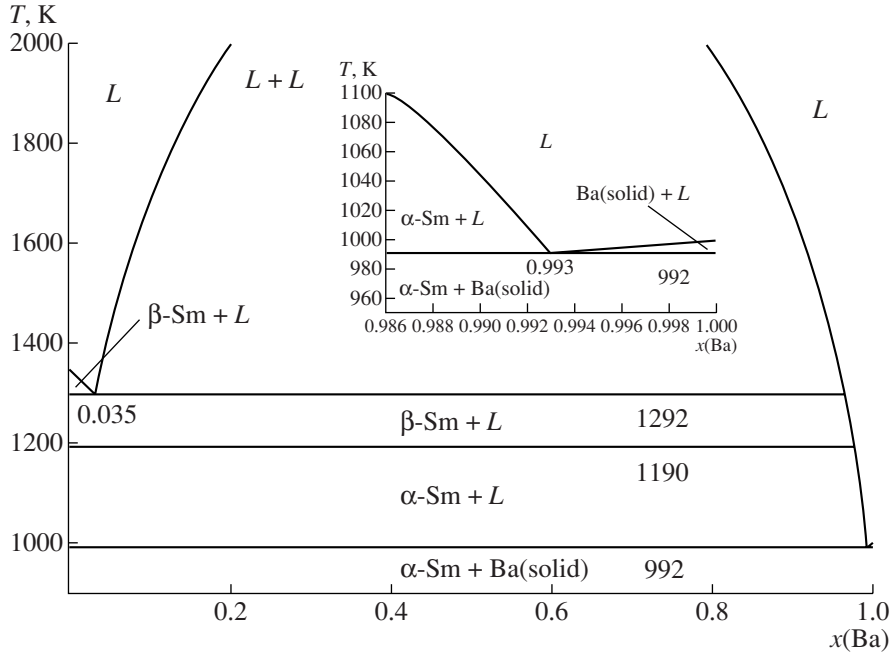

Fig. 3. Sm–Ba phase diagram.

ditions for condensed phases. Equilibrium at the monotectic point of an Ln–Ba system is, for example,

$$\mathrm{Ln}_{1-x_a}\mathrm{Ba}_{x_a}(\mathrm{liq}) = \left(1-\frac{x_a}{x_b}\right)\mathrm{Ln}(\mathrm{solid}) + \frac{x_a}{x_b}\mathrm{Ln}_{1-x_b}\mathrm{Ba}_{x_b}(\mathrm{liq}),$$

where x_a and x_b are, respectively, the mole fractions of the second component (in the case at hand, barium) in equilibrium liquid phases rich in the first and second component (lanthanide and barium). Three phases coexisting in equilibrium at an invariant point, the following three equalities must hold simultaneously:

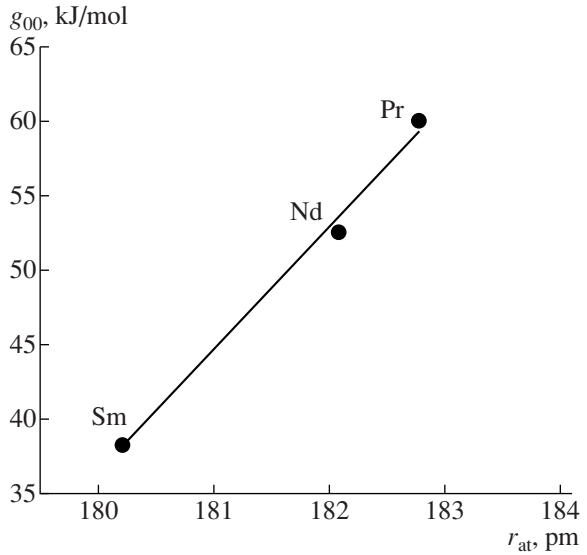

Fig. 4. g_{00} vs. lanthanide atomic radius.

$$\begin{cases} \dfrac{x_a}{x_b}\Delta_{\text{mix}}G(x_b) - \Delta_{\text{mix}}G(x_a) - \left(1 - \dfrac{x_a}{x_b}\right)\Delta_m G^\circ_{\text{Ln}}(T) = 0 \\ -\Delta_m G^\circ_{\text{Ln}}(T) = RT\ln(1-x_a) + \mu^{\text{ex}}_{\text{Ln}}(x_a) \\ -\Delta_m G^\circ_{\text{Ln}}(T) = RT\ln(1-x_b) + \mu^{\text{ex}}_{\text{Ln}}(x_b), \end{cases}$$

Here, $\Delta_m G^\circ_{\text{Ln}}(T)$ is the Gibbs energy of melting for the lanthanide, $\Delta_{\text{mix}}G(x)$ is the Gibbs energy of melt mixing, and $\mu^{\text{ex}}_{\text{Ln}} = g_{00}x^2$ is the excess chemical potential of the lanthanide in melt.

Results and Discussion

The PhDi program, used to find the parameter g_{00} in the modeling of the liquid and design of the Ln–Ba phase diagrams, was developed at the Chemical Thermodynamics Laboratory, Faculty of Chemistry, Moscow State University; a demo version of this program is available from http://td.chem.msu.su/. Table 3 and Figs. 1–3 display the results of the calculations. The stability parameters and phase-transition temperatures of the components were borrowed from [11]. In all calculations, the barium melting point was set to be 1000 K.

In order to estimate the parameter g_{00} for the Gd–Ba system, we plotted g_{00} as a linear function of lanthanide atomic radius for Ln = Sm, Nd, and Pr (Fig. 4):

$$g_{00}(\pm 1300)\ \text{J/mol} = -(1.437 \pm 0.124) \times 10^6 + (8184 \pm 680)r_{\text{at}}(\text{pm}).$$

The gadolinium atomic radius being 180.2 pm, we found the interaction parameter for Gd–Ba melts:

$$g_{00} = (37760 \pm 1300)\ \text{J/mol}.$$

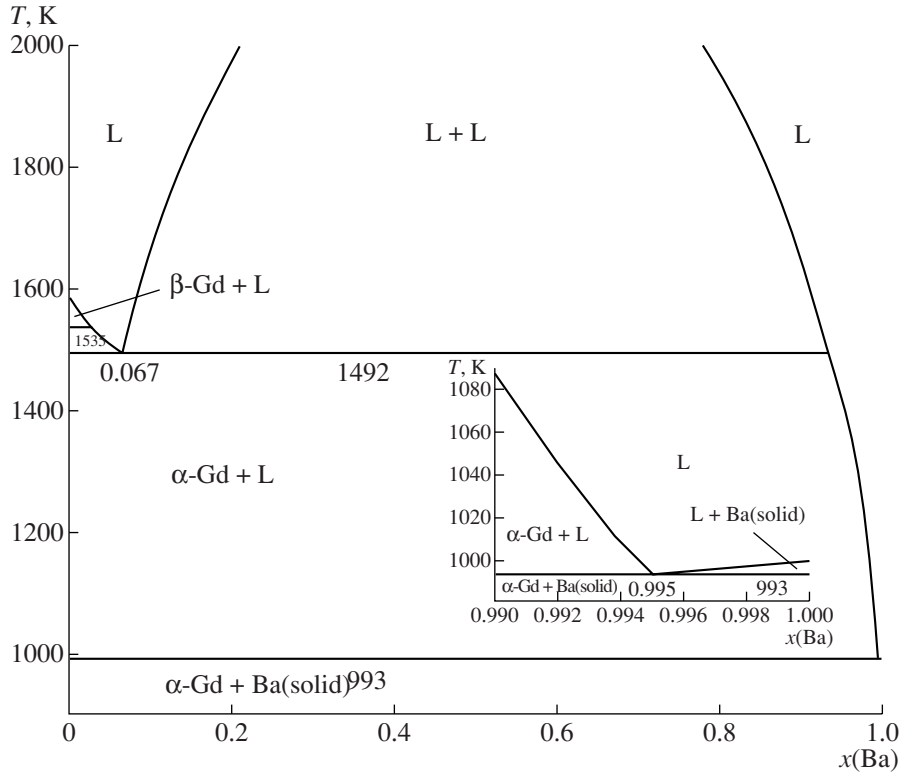

Fig. 5. Gd–Ba phase diagram.

The thermodynamic model was used to calculate the Gd–Ba phase diagram as shown in Fig. 5. The diagram features an exsolution dome, a monotectic at 1492 K and 6.7 at % Ba, and a eutectic at 993 K and 99.5 at % Ba. The gadolinium melting temperature and the α-Gd ⟶ β-Gd phase-transition temperature was set to be 1587 and 1535 K, respectively.

ACKNOWLEDGMENTS

This work was supported by the Russian Foundation for Basic Research (project nos. 05-03-32960 and 05-03-32963) and the Program for Support of Leading Scientific Schools (grant no. NSh7022.2006.3).

REFERENCES

1. Rudnyi, E.B. and Voronin, G.F., *CALPHAD: Comput. Coupling Phase Diagrams Thermochem.*, 1996, vol. 20, p. 297.
2. Lysenko, V.A., Kuz'menko, V.V., Uspenskaya, I.A., Rudnyi, E.B., and Voronin, G.F., *Zh. Ross. Khim. O–va im. D.I. Mendeleeva*, 2001, vol. 45, no. 3, p. 86.
3. Lysenko, V.A., *Zh. Fiz. Khim.*, 2003, vol. 77, p. 1556.
4. Lysenko, V.A., *Zh. Fiz. Khim.*, 2004, vol. 78, p. 223.
5. Pyagai, I.N., Khairudinov, S.Kh., and Vakhobov, A.V., *Izv. Akad. Nauk SSSR, Met.*, 1986, no. 3, p. 216.
6. Griffin, R.B. and Gscheneidner, K.A., (Jr.), *Metall. Trans. A*, 1971, vol. 2, p. 2517.
7. Eshonov, K.K., Zukhuritdinov, M.A., Vakhobov, A.V., and Dzhuraev, T.D., *Izv. Akad. Nauk SSSR, Met.*, 1978, no. 1, p. 191.
8. Menshchikova, O.A., Vakhobov, A.V., and Dzhuraev, T.D., *Izv. AN Tadzh. SSR. Otd. Fiz.-Mat. Geol.-Khim. Nauk*, 1977, no. 3(65), p. 191.
9. Gshneidner, K.A. (Jr.) and Calderwood, F.W., *Bull. Alloy Phase Diagrams*, 1988, vol. 9, no. 3. p. 218.
10. Emsley, J., *The Elements*, London, 1990.
11. Dinsdale, A.T., *CALPHAD: Comput. Coupling Phase Diagrams Thermochem.*, 1991, vol. 15, p. 317.